Equilibrium Se isotope fractionation parameters: A first-principles study

Xuefang Li, Yun Liu *

State Key Laboratory of Ore Deposit Geochemistry, Institute of Geochemistry, Chinese Academy of Sciences, Guiyang 550002, China

ABSTRACT

Several important equilibrium Se isotope fractionation parameters are investigated by first-principles calculations, involving dominant inorganic and organic Se-bearing species in gaseous, aqueous and condensed phases. Because anharmonic effects are found to be negligible for Se isotope fractionation calculation, the Bigeleisen–Mayer equation method is used without corrections beyond harmonic approximation. All calculations are made at B3LYP/6-311 + G(d,p) level, with a frequency scaling factor of 1.05. Solvation effects are carefully evaluated by the explicit solvent model (i.e. the "water droplet" method). A number of conformers are used for aqueous complexes in order to reduce the possible error coming from different configurations.

Redox state is found to be an important factor controlling equilibrium Se isotope fractionations. Our results suggest a trend of heavy Se isotopes enrichment as $SeO_4^{2-} > SeO_3^{2-} > HSeO_3^- > SeO_2 >$ selenoamino acids> alkylselenides> Se(0) or $H_2Se > HSe^-$. The Se(−II) species regardless of organic and inorganic forms can enrich extremely light Se isotopes comparing with other species. Equilibrium Se isotope fractionation factors provided in this study suggest Se isotopes can be used as a tracer of redox conditions and also useful to study Se cycling.

© 2011 Elsevier B.V. All rights reserved.

1. Introduction

Selenium (Se) is an indispensable trace element for human and animals. Meanwhile, Se is also toxic due to excessive intake. Similar to sulfur (S), Se usually exists in several valence states, including +VI, +IV, +II, 0, and −II states in inorganic and organic compounds under different redox environments. Several previous studies (Dauchy et al., 1994; Hashimoto and Winchester, 1967; Johnson, 2004; Wen and Carignan, 2007) described the forms of Se species in different phases. In the atmosphere, inorganic compounds include H_2Se, Se_2, SeO and SeO_2, while single molecule is instable and easily transforms into particulate phase. Dimethyl Se (DMSe) (i.e. CH_3SeCH_3) (Challenger and North, 1934) is the major species in volatile organic matters, in addition, dimethyl diselenide (DMDSe) (i.e. $CH_3SeSeCH_3$), dimethyl selenenyl sulfide (DMSeS) (i.e. CH_3SeSCH_3) and other alkylselenides were also identified in the atmosphere, natural aqueous systems and particulate phase despite of their small contents (Dauchy et al., 1994). The stable aqueous Se species mainly depend on redox conditions (Cutter, 1982; Elrashidi et al., 1987; Johnson and Bullen, 2004), selenate (SeO_4^{2-}) is the dominate anion under oxidizing conditions, and it can be reduced to selenite (SeO_3^{2-}) and biselenite ($HSeO_3^-$) under mildly reducing conditions, moreover it can be also reduced to Se(0) under moderately reducing conditions. If under strongly reducing conditions, only Se(−II) species may exist. In the oceans, Se(VI), Se(IV) and organic Se are dominate species, but the inorganic species will be decreased in surface waters because of biological assimilation processes, and organic Se(II) complexes, for example, Se-amino acids, hold a leading pose (McConnell and Wabnitz, 1957; Peterson and Butler, 1962). In a condensed phase, elemental Se has been widely discovered in nature (Sun and Weege, 1959; Thompson et al., 1956; Zhu et al., 2002, 2004, 2005), and its crystal forms are diverse, including trigonal, monoclinic structures, etc. Se concentration in the Earth's crust is around below 0.5 μg/g (Rouxel et al., 2002). Se in most rocks is less than 0.1 ppm, but shale is an exception with about 1 ppm. Coal is also an important Se reservoir with an average of 3 ppm (Cooper et al., 1974).

Se has six stable isotopes, [74]Se, [76]Se, [77]Se, [78]Se, [80]Se, and [82]Se, with relative abundances of 0.889%, 9.366%, 7.635%, 23.772%, 49.607% and 8.731%, respectively (Johnson and Bullen, 2004). Because Se belongs to one of the most redox-sensitive elements (Fan et al., 2007), and the mass differences between its isotopes (such as between [76]Se and [82]Se) are large, Se isotopes were expected to have large fractionations in nature. Previous studies suggested that the largest Se isotopic variation (in terms of $\delta^{82/76}Se_{NIST}$ values) varied from −12.77‰ to 4.93‰ (Johnson et al., 1999; Rouxel et al., 2002; Wen et al., 2007). Se isotopes are distinctively fractionated in a number of geologic processes and they are good candidates as tracers of redox and bio-interference processes.

There are just a few pioneering studies that provided equilibrium Se isotope fractionation factors. Krouse and Thode (1962) measured

* Corresponding author. Tel.: +86 851 5890798; fax: +86 851 5891664.
E-mail address: liuyun@vip.gyig.ac.cn (Y. Liu).

normal vibrational spectra of some Se-containing compounds and used the Bigeleisen–Mayer equation method (Bigeleisen and Mayer, 1947; Urey, 1947) to calculate equilibrium fractionation factors among several Se isotope systems for the first time. Schauble (2004) used the spectroscopic data of Krouse and Thode (1962) and the empirical force field to produce fractionation factors for several gaseous Se molecules. Due to the lack of spectroscopic data, many important Se isotope systems were not included in these previous studies. Furthermore, several important Se aqueous species were simply treated as gaseous molecules without considering solvation effects. Such treatment might bring large errors to Se isotope fractionation calculations. Therefore, precise equilibrium Se isotope fractionation factors of many important geological systems are still not well established.

In this study, SeO_2, SeO, Se_2, H_2Se, DMSe, DMDSe and DMSeS in gaseous phase, SeO_4^{2-}, SeO_3^{2-}, $HSeO_3^-$, HSe^-, two Se-amino acids, Selenomethionine (SeMet) and selenocystine (SeCyst) in aqueous phase, and monoclinic and trigonal elemental Se in solid phase are chosen as important geological Se isotope systems for studying. These basic isotope fractionation parameters are expected to provide important information for the Se stable isotope geochemistry field.

2. Methods

2.1. Bigeleisen–Mayer equation or Urey model

The Bigeleisen–Mayer equation (hereafter, B–M equation) or the Urey model has been the cornerstone of stable isotope geochemistry for decades (Bigeleisen and Mayer, 1947; Urey, 1947). Readers are referred to several reviews of this method for further information (Chacko et al., 2001; Criss, 1999; O'Neil, 1986; Richet et al., 1977; Schauble, 2004).

For an isotope exchange reaction between substances A and B,

$$A + B^* \leftrightarrow A^* + B \tag{1}$$

where the asterisk represents the substance with heavier isotopes. The reaction equilibrium constant K_{A-B} is related to the isotope fractionation factor α_{A-B} ($\alpha = K^{1/n}$ if the excess factor is ignored). n is the number of isotopes exchanged. In this study, we only consider situations with $n = 1$ (only one isotope exchanged). Based on statistical mechanics, K_{A-B} can be expressed by

$$K_{A-B} = \frac{(Q^*)_A (Q)_B}{(Q)_A (Q^*)_B} = \frac{(Q^*/Q)_A}{(Q^*/Q)_B} \tag{2}$$

where Q is the total partition function of substance A or B, and equals to the product of a series of subgroup of partition functions such as electronic (Q_{elec}), translational (Q_{tran}), rotational (Q_{rot}), and vibrational (Q_{vib}) partition functions, etc. If pure harmonic frequencies are used, the Teller–Redlich product rule (Redlich, 1935) is often employed to further simplify the calculation procedure, and consequently the mass-weighted reduced isotope partition function ratios (RPFR for short) are used instead of the original partition function ratios:

$$RPFR = \prod_i^N \frac{u_i^* \exp(-u_i^*/2)[1 - \exp(-u_i)]}{u_i \exp(-u_i/2)[1 - \exp(-u_i^*)]} \tag{3}$$

and

$$K_{A-B} = \frac{\left(\frac{s}{s^*}\right)_A}{\left(\frac{s}{s^*}\right)_B} \frac{RPFR(A^*/A)}{RPFR(B^*/B)} \tag{4}$$

where s is the symmetry number of the molecule; N is the harmonic vibrational modes of the molecule ($3n - 6$ for non-linear, polyatomic

molecules or $3n - 5$ for linear, polyatomic molecules consisting of n atoms), and

$$u_i = \frac{h v_i}{kT} \tag{5}$$

where v_i denotes the ith vibrational frequency; h is Planck's constant; k is Boltzmann's constant and T is temperature in Kelvin. Therefore, RPFR only relates to the harmonic vibrational frequencies before and after the isotope substitution. Geochemists often use β factor instead of RPFR because $\alpha = \beta_A/\beta_B$. The β factor will equal to the RPFR value when there is only one isotope exchanged.

2.2. Calculation details

The number of stable isotope geochemistry studies using computational quantum chemistry methods is increasing rapidly (e.g. Anbar et al., 2005; Driesner and Seward, 2000; Jarzecki et al., 2004; Li and Liu, 2010; Liu and Tossell, 2005; Liu et al., 2010; Oi, 2000; Oi and Yanase, 2001; Otake et al., 2008; Rustad and Bylaska, 2007; Rustad and Zarzycki, 2008; Rustad et al., 2008, 2010; Schauble, 2004, 2007; Schauble et al., 2003, 2006; Seo et al., 2007; Zeebe, 2005, 2010). The key point of this kind of calculation is obtaining precise harmonic frequencies of interested isotope systems. Computational quantum chemistry methods can provide harmonic frequencies easily (Harris, 1995; Hehre et al., 1986).

In this study, geometry optimizations and frequency calculations are implemented at B3LYP/6-311 + G(d,p) level using GAUSSIAN03 software package (Frisch et al., 2003). The hybrid DFT method, B3LYP (Becke, 1993; Lee et al., 1988) is one of the most popular methods for vibrational frequency calculation. Triple-zeta basis-set 6-311 + G(d,p) is chosen because Se is a third-row element and we used this basis-set to successfully handle Ge isotope fractionations (Li and Liu, 2010; Li et al., 2009), which is very similar to the Se case. Because the B3LYP/6-311 + G(d,p) level underestimates vibrational frequencies in Ge isotope calculation, moreover, this is a common phenomenon for *ab initio* calculations and especially for heavy elements in solution with extra charges (Li et al., 2009). Here, for the Se isotope fractionation calculation, the scaling factor 1.05 also makes harmonic frequencies close to those at MP2/aug-cc-pVTZ, CCSD/aug-cc-pVTZ and CCSD/aug-cc-pVQZ levels which are usually considered as precise ones for harmonic frequencies (see Table A1 in the Appendix). Therefore, we also choose 1.05 as frequency scaling factor in this study to remedy the inadequacy of the theoretical level.

To check the possible effects of higher-order corrections to the B–M equation beyond harmonic levels (Liu et al., 2010), a series of higher-order corrections are evaluated for H_2Se (Table 1). Detailed formalism about these higher-order corrections can be found in Liu et al. (2010). At the B3LYP/6-311 + G(d,p) level with a frequency scaling factor of 1.05, the differences between the uncorrected and corrected RPFR are about 0.2‰ for two different initial structures of H_2Se (Table 1), suggesting that the anharmonic effect for Se isotopes is not significant even for a H-bearing small molecule. Considering the

Table 1
The anharmonic correction to RPFR results of H_2Se.

	RPFR	AnZPE	AnEXC	AnCorr	AnRPFR	Diff (‰)
H_2Se_A	1.005609	1.0001597	1.0000015	1.0001612	1.005771	0.2
H_2Se_B	1.005611	1.0001526	1.0000015	1.0001542	1.005766	0.2

Note: A and B represent two different initial structures of H_2Se; RPFR is reduced partition function ratio based on the Bigeleisen–Mayer equation; AnZPE is the anharmonic correction for the zero-point energy (e.g. $AnZPE = Q_{AnZPE}^*/Q_{AnZPE}$); AnEXC is the anharmonic correction for the vibrational excited states; AnCorr is the product of AnZPE and AnEXC; AnRPFR is the product of RPFR and AnCorr; Diff is the difference between AnRPFR and RPFR.

huge computing cost of many large Se systems studied here, we choose not to include the calculation of these higher-order corrections at this time.

All aqueous Se species are modeled using the explicit solvent model, so-called the "water-droplet" method, which solvent water molecules are added surrounding the species of interest to simulate solution environment. The explicit solvent model has been used to treat a lot of aqueous species in solutions (Driesner and Seward, 2000; Li et al., 2009; Liu and Tossell, 2005; Rustad et al., 2008), and has showed reliable results. For reducing possible errors caused by different configurations, every aqueous Se species is evaluated by adding different numbers of water molecules (i.e. 6, 12, 18, and 24, respectively) and each "water-droplet" cluster is optimized twice from two different initial structures (A and B). Finally, the average RPFR value of the Se species with 12, 18 and 24 water molecules is taken (as the preferred value in Table 2).

3. Results

3.1. Se species in gaseous phase

Structures of the dominant inorganic Se species SeO_2, SeO, Se_2, and H_2Se (Fig. 1a–d) in the atmosphere are studied. The H–Se–H bond angle of H_2Se is 91° (Fig. 1d) and the bond length of Se–H is 1.47 . They are consistent with known experimental data. In Table 2, the comparison of calculated harmonic, calculated fundamental and experimental fundamentals for SeO (Hezberg, 1950) and H_2Se (Cameron et al., 1939) are given. The calculated fundamental frequencies can generally match the experimental ones. Several volatile alkylselenides, e.g. DMSe, DMDSe and DMSeS, are also calculated. Optimized geometries are shown in Fig. 1e–g. RPFRs of these species in terms of $^{82}Se/^{76}Se$ at 25 °C are shown in Table 3.

Schauble (2004) had calculated the β factors (denoted as α_{AX-X} in his paper) of several gaseous Se-bearing molecules based on measured vibrational spectra (Krouse and Thode, 1962). Our results, which are purely based on quantum chemistry calculations, are very close to his results. Such as, his β factors of H_2Se, Se_2, and SeO are 1.005, 1.0055 and 1.008 at 298.15 K, respectively, comparing to our results (1.0056, 1.0056 and 1.0084). Note that the β factor of Se_2 listed in his paper was not for singly substituted situation. We correct it into the right way here (i.e. 1.011 is changed to 1.0055).

3.2. Se species in aqueous phase

According to the Eh–pH stability diagram given by Johnson and Bullen (2004), the highly soluble inorganic species SeO_4^{2-}, SeO_3^{2-} or $HSeO_3^-$ can generally co-exist in nature waters and most of soils. In reducing waters, HSe^- is the stable inorganic form. Therefore, isotope
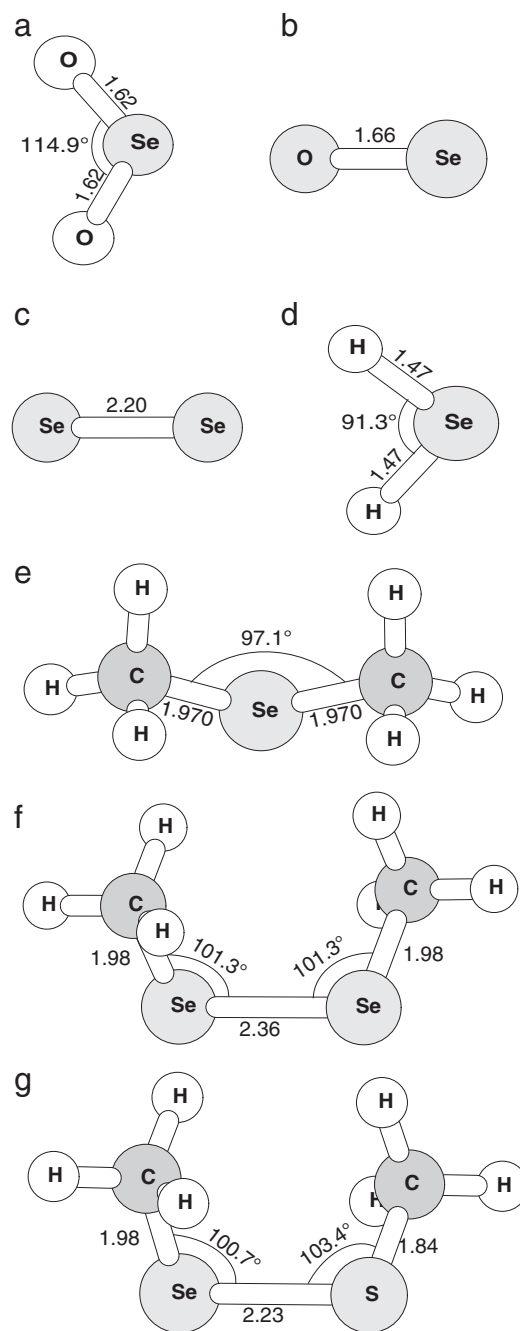

Fig. 1. Several gaseous Se molecules: (a) SeO_2; (b) SeO; (c) Se_2; (d) H_2Se; (e) DMSe; (f) DMDSe; and (g) DMSeS. Bond lengths are in Angstrom (Å) in this paper.

fractionation factors among these aqueous Se species are very important for the study of Se isotope distribution in solutions.

Here, SeO_4^{2-}, SeO_3^{2-}, $HSeO_3^-$ and HSe^- with different numbers (i.e. 6, 12, 18 and 24) of water molecules are optimized and performed frequency calculations. No imaginary frequency is found, meaning their structures are optimized to the energy minimum points. Optimized structures with 24 water molecules are shown in Fig. 2a–d, respectively. Two different configurations (A and B) for every water-droplet are calculated from different starting structures (Table 3). The preferred RPFR is the average value of water-droplets with 12, 18, and 24 water molecules. The preferred RPFR values of SeO_4^{2-}, SeO_3^{2-}, $HSeO_3^-$ and HSe^- are shown in Table 3.

Under reducing conditions, especially in shallow surface waters, Se-bearing organic compounds will be significantly increased because of biological uptake and assimilation, and become the predominant

Table 2
The comparison of calculated harmonic, calculated fundamental and experimental fundamental frequencies of two gaseous Se molecules at B3LYP/6-311 + G** level.

	Molecule			
	SeO		H_2Se	
Calc. harmonic frequencies (no scaling) (cm^{-1})	891	1072	2378	2394
Calc. harmonic frequencies (scaled by 1.05) (cm^{-1})	935	1125	2496	2514
Calc. fundamentals (cm^{-1})*	884	1033	2445	2447
Experimental fundamentals(cm^{-1})	897.9	1074	2260	2350

Note: The calculated fundamental frequency (v_i) is obtained from

$$v_i = \omega_i + 2x_{ii} + \frac{1}{2}\sum_{i \neq j} x_{ij}$$

where ω_i is the harmonic frequency and x_{ij} is the anharmonic constant (e.g. Barone, 2004).

Table 3
RPFR results in term of $^{82}Se/^{76}Se$ for Se species in gaseous, liquid, and condense phases at B3LYP/6-311 + G(d,p) level, with a frequency scaling factor of 1.05 (25 °C).

Species	RPFR	Species	RPFR	Species	RPFR
Gaseous phase					
SeO_2	1.02003	SeO	1.00843	H_2Se	1.00561
Se_2	1.00562	CH_3SeCH_3	1.00999	CH_3SeSCH_3	1.00872
$CH_3SeSeCH_3$	1.00833				
Liquid phase					
SeO_4^{2-}	1.035038	SeO_3^{2-}	1.022453	$HSeO_3^-$	1.023188
$SeO_4^{2-}-6H_2O\_A$	1.036819	$SeO_3^{2-}-6H_2O\_A$	1.023415	$HSeO_3^--6H_2O\_A$	1.023593
$SeO_4^{2-}-6H_2O\_B$	1.036826	$SeO_3^{2-}-6H_2O\_B$	1.023645	$HSeO_3^--6H_2O\_B$	1.023841
$SeO_4^{2-}-12H_2O\_A$	1.037314	$SeO_3^{2-}-12H_2O\_A$	1.023872	$HSeO_3^--12H_2O\_A$	1.023369
$SeO_4^{2-}-12H_2O\_B$	1.037410	$SeO_3^{2-}-12H_2O\_B$	1.023848	$HSeO_3^--12H_2O\_B$	1.023598
$SeO_4^{2-}-18H_2O\_A$	1.037697	$SeO_3^{2-}-18H_2O\_A$	1.024012	$HSeO_3^--18H_2O\_A$	1.023715
$SeO_4^{2-}-18H_2O\_B$	1.037862	$SeO_3^{2-}-18H_2O\_B$	1.024075	$HSeO_3^--18H_2O\_B$	1.023875
$SeO_4^{2-}-24H_2O\_A$	1.038032	$SeO_3^{2-}-24H_2O\_A$	1.024244	$HSeO_3^--24H_2O\_A$	1.023630
$SeO_4^{2-}-24H_2O\_B$	1.038291	$SeO_3^{2-}-24H_2O\_B$	1.024341	$HSeO_3^--24H_2O\_B$	1.023166
Preferred value[*]	1.03777	Preferred value[*]	1.02407	Preferred value[*]	1.02356
HSe^-	1.002314	SeMet	1.010001	SeCyst	1.009972
$HSe^--6H_2O\_A$	1.003666	$SeMet-6H_2O\_A$	1.010348	$SeCyst-6H_2O\_A$	1.010041
$HSe^--6H_2O\_B$	1.003657	$SeMet-6H_2O\_B$	1.010301	$SeCyst-6H_2O\_B$	1.010191
$HSe^--12H_2O\_A$	1.003879	$SeMet-12H_2O\_A$	1.010321	$SeCyst-12H_2O\_A$	1.010118
$HSe^--12H_2O\_B$	1.003915	$SeMet-12H_2O\_B$	1.010271	$SeCysta-12H_2O\_B$	1.010086
$HSe^--18H_2O\_A$	1.004661	$SeMet-18H_2O\_A$	1.010459	$SeCyst-18H_2O\_A$	1.010215
$HSe^--18H_2O\_B$	1.004702	$SeMet-18H_2O\_B$	1.010338	$SeCyst-18H_2O\_B$	1.010206
$HSe^--24H_2O\_A$	1.004493	$SeMet-24H_2O\_A$	1.010641	$SeCyst-24H_2O\_A$	1.010521
$HSe^--24H_2O\_B$	1.004601	$SeMet-24H_2O\_B$	1.010485	$SeCyst-24H_2O\_B$	1.010616
Preferred value[*]	1.00438	Preferred value[*]	1.01042	Preferred value[*]	1.01030
Condensed phase					
Se(monoclinic)[1]	1.006061			Se(trigonal)	1.00595
Se(monoclinic)[2]	1.006023				
Se(monoclinic)[3]	1.005976				
Se(monoclinic)[4]	1.005978				
average value	1.00601				

The superscripts 1, 2, 3 and 4 denote the monoclinic structures where different position Se atoms are exchanged.
[*] The average RPFR value from clusters with 12, 18, and 24 water molecules.

species. Many studies proposed the model of Se biogeochemical cycling in aquatic phase (Cooke and Bruland, 1987; Fan et al., 2002; Flury et al., 1997; Frankenberger and Arshad, 2001; Suzuki et al., 2008). The simplified schematic diagram can be found in Fig. 6 in the paper of Cooke and Bruland (1987). The reductive assimilation of selenate and selenite by an organism in these processes is the main reason of production of selenoamino acids. Several investigations confirmed the occurrence of selenoamino acids, such as SeMet (Kajander et al., 1989; McConnell and Wabnitz, 1957) and SeCyst (Martin and Gerlach, 1969; McConnell and Wabnitz, 1957; Peterson and Butler, 1962).

Here, SeMet and SeCyst are calculated using the water-droplet method. Optimized clusters surrounding 24 water molecules are shown in Fig. 2e and f. The preferred RPFR values of SeMet and SeCyst are also shown in Table 3.

3.3. Elemental Se in condensed phase

Elemental Se can exist in trigonal, monoclinic, orthorhombic and cubic crystals, but only trigonal Se is the most stable form at usual conditions. Other crystal systems are apt to convert into the trigonal form. The monoclinic elemental Se includes α and β types of structures. The two structures consist of a number of crown-like Se_8 rings, with high similarity (Burbank, 1951, 1952; Marsh et al., 1953). The Se isotope fractionation between these two monoclinic structures is negligible. Therefore, we only build two models to study elemental Se, one for monoclinic Se (Fig. 3a) and the other for trigonal Se (Fig. 3b). The two models are directly cut from X-ray structures of elemental Se crystals and it is a common treatment of using cluster model to study minerals (Gibbs, 1982; Liu and Tossell, 2005; Rustad and Zarzycki, 2008; Rustad et al., 2008).

For the monoclinic Se, the initial structure is from X-ray coordinates of β-Se determined by Marsh et al. (1953), with a = 12.85 , b = 8.07 , c = 9.31 , α = 90.0°, β = 93.1°, and γ = 90.0° in unit cell, and space group P121/a1(Marsh et al., 1953). The positions of 5 Se atoms are fixed (Se atom No. 3–7 in Fig. 3a) in the Se_8 ring in order to keep the monoclinic form of structure. Three Se atoms (Se1, Se2 and Se8 in Fig. 3a) are freely optimized. The middle Se atom in gray color (Se1) is the one with exchanged isotopes. Alternatively, we calculate 4 different exchange positions of Se atoms in the Se_8 ring (Fig. 3a is just one of them). Although we find that position difference in this Se_8 ring has almost no effect on RPFR (Table 3), we still use the average value of the four different positions as the preferred RPFR of monoclinic Se (1.00601) at 298.15 K.

For trigonal Se, the initial structure is from X-ray coordinates determined by Cherin and Unger (1967). The parameters of the unit cell are a = 4.3662 , c = 4.9536 , α = β = 90.0°, and γ = 120.0° and the space group is P3$_1$21. We fixed the atoms in the outer-most layer in order to avoid breaking down during optimization (Fig. 3b). Although there are a few imaginary frequencies produced, they are all very small ones (<60 cm^{-1}). According to our experiences, they reflect false measurements of weak interactions after geometry optimization and cannot contribute significant changes to a "true" RPFR result. Therefore, they can be safely neglected. The RPFR value of trigonal Se is very close to that of monoclinic Se (Table 3) though their structures are quite different. It is because both of them are at Se(0) valence state and also with the same Se–Se bonding.

3.4. Equilibrium Se isotope fractionations

Equilibrium Se isotope fractionation factor α_{A-B} can be obtained easily between any two Se species studied. The "per mil" fractionation
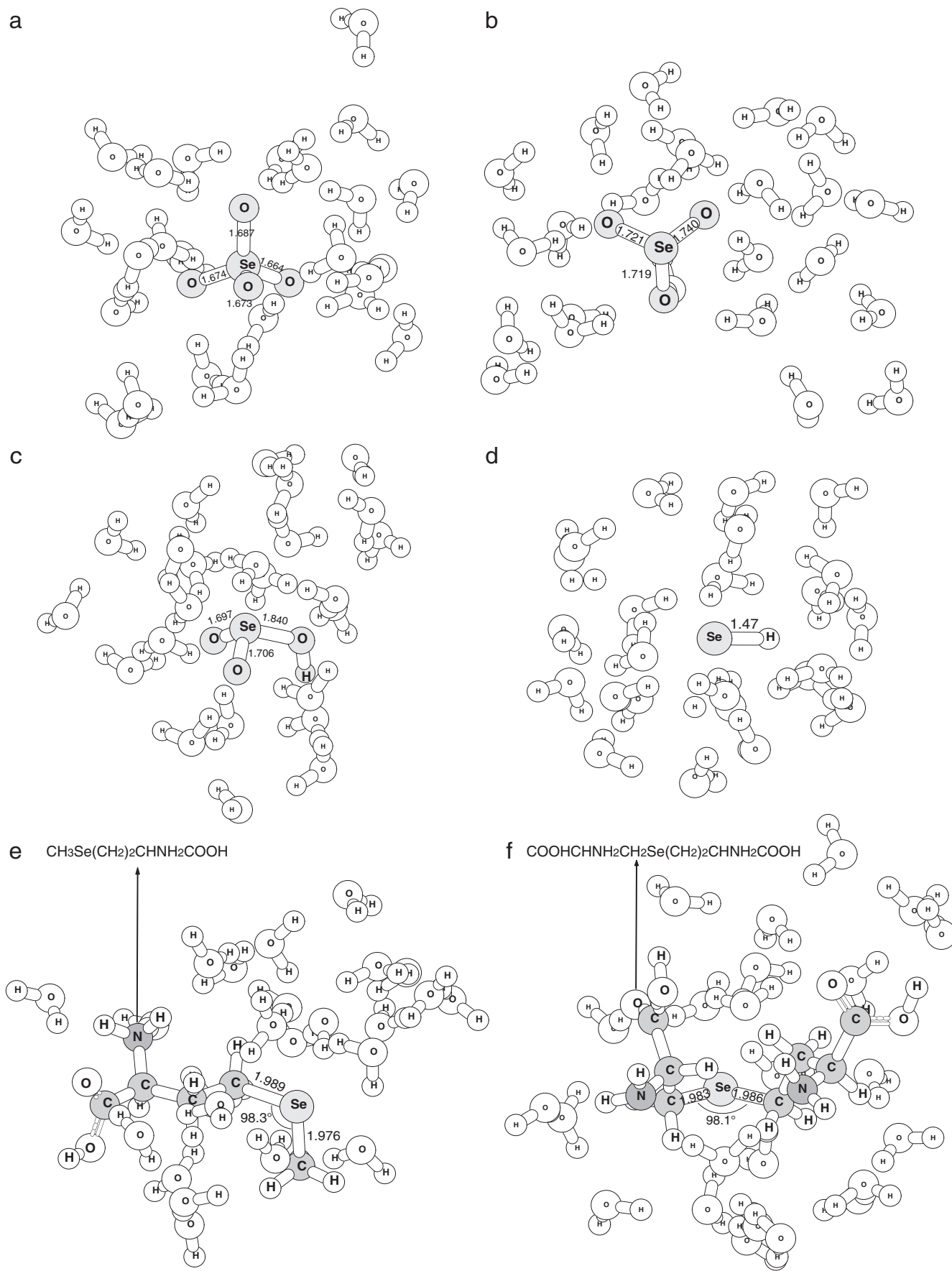
Fig. 2. Cluster models of aqueous Se species with 24 water molecules. (a) SeO_4^{2-}; (b) SeO_3^{2-}; (c) $HSeO_3^{-}$; (d) HSe^{-}; (e) Selenomethionine; and (f) selenocystine.
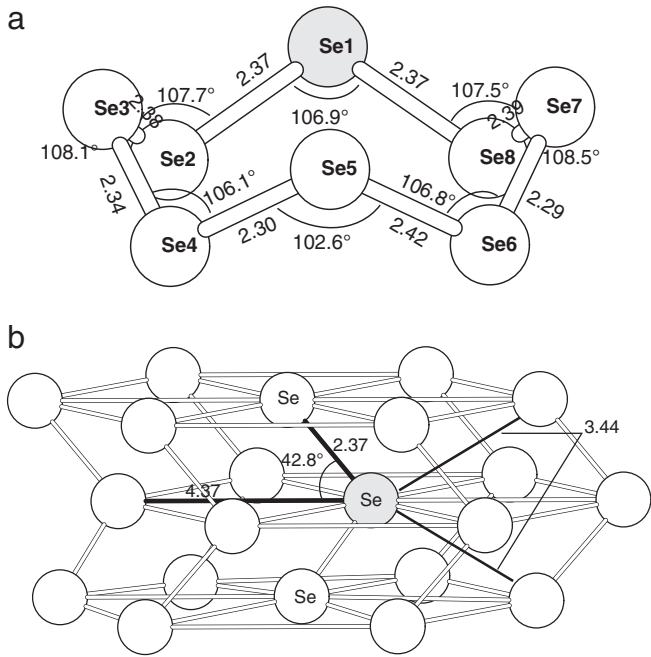
a

b

Fig. 3. Cluster models for elemental Se (a) monoclinic Se; (b) trigonal Se. Se atom in gray color denotes the exchanged one.

$\Delta_{A-B} (\approx 10^3 \ln\alpha)$ data are shown in Table 4. These results suggest a trend of heavy Se isotope enrichment as $SeO_4^{2-} > SeO_3^{2-} > HSeO_3^- > SeO_2 >$ selenoamino acids > alkylselenides > Se(0) or $H_2Se > HSe^-$. Again, redox conditions play an important role in controlling Se isotope fractionation.

Table 5
The formula for Se isotope fractionations at different temperatures.

A–B	$10^3\ln(\alpha_{A-B}) = a \ 10^6/T^2 + b \ 10^3/T + c$
$SeO_4^{2-}-SeO_3^{2-}$	$10^3\ln(\alpha_{A-B}) = 0.524637 \ 10^6/T^2 + 2.94785 \ 10^3/T - 2.50587$
$SeO_4^{2-}-HSeO_3^-$	$10^3\ln(\alpha_{A-B}) = 0.608479 \ 10^6/T^2 + 2.77841 \ 10^3/T - 2.38642$
$SeO_4^{2-}-HSe^-$	$10^3\ln(\alpha_{A-B}) = 1.709258 \ 10^6/T^2 + 5.51101 \ 10^3/T - 5.02758$
$SeO_3^{2-}-HSeO_3^-$	$10^3\ln(\alpha_{A-B}) = 0.083841 \ 10^6/T^2 - 0.16944 \ 10^3/T + 0.11944$
$SeO_3^{2-}-HSe^-$	$10^3\ln(\alpha_{A-B}) = 1.184621 \ 10^6/T^2 + 2.56316 \ 10^3/T - 2.52171$
$SeO_4^{2-}-SeMet$	$10^3\ln(\alpha_{A-B}) = 1.236799 \ 10^6/T^2 + 5.12772 \ 10^3/T - 4.42211$
$SeO_4^{2-}-SeCyst$	$10^3\ln(\alpha_{A-B}) = 1.204255 \ 10^6/T^2 + 5.32442 \ 10^3/T - 4.59242$
$SeO_4^{2-}-DMSe$	$10^3\ln(\alpha_{A-B}) = 1.323029 \ 10^6/T^2 + 4.90539 \ 10^3/T - 4.22539$
$SeO_4^{2-}-DMDSe$	$10^3\ln(\alpha_{A-B}) = 1.306259 \ 10^6/T^2 + 5.48531 \ 10^3/T - 4.72162$
SeO_2-SeO	$10^3\ln(\alpha_{A-B}) = 0.438882 \ 10^6/T^2 + 2.57817 \ 10^3/T - 2.15291$
SeO_2-Se_2	$10^3\ln(\alpha_{A-B}) = 0.335359 \ 10^6/T^2 + 4.14586 \ 10^3/T - 3.45764$
SeO_2-H_2Se	$10^3\ln(\alpha_{A-B}) = 0.725619 \ 10^6/T^2 + 2.61754 \ 10^3/T - 2.71278$
$SeO_2-Se(T)$	$10^3\ln(\alpha_{A-B}) = 0.263308 \ 10^6/T^2 + 4.34169 \ 10^3/T - 3.63616$
$SeO_2-Se(M)$	$10^3\ln(\alpha_{A-B}) = 0.257529 \ 10^6/T^2 + 4.34519 \ 10^3/T - 3.63933$
$SeO-Se(T)$	$10^3\ln(\alpha_{A-B}) = -0.175574 \ 10^6/T^2 + 1.76352 \ 10^3/T - 1.48325$
SeO_2-DMSe	$10^3\ln(\alpha_{A-B}) = 0.198796 \ 10^6/T^2 + 3.02243 \ 10^3/T - 2.49061$
$SeMet-DMSe$	$10^3\ln(\alpha_{A-B}) = 0.086231 \ 10^6/T^2 - 0.22233 \ 10^3/T + 0.19672$

Our gaseous Se species results agree with those of Krouse and Thode (1962) and Schauble (2004) very well, which are based on experimental vibrational spectra data. Except for gaseous Se species, we also provide a lot of basic and important Se fractionation factors related to aqueous Se species, organic Se species and elemental Se. These data are crucial for many Se stable isotope geochemistry studies.

In addition, we provide Se isotope fractionation factors at different temperatures in Table 5. A simple $10^3\ln(\alpha) = a^*10^6/T^2 + b^*10^3/T + c$ formula is used to facilitate the calculation of Se isotope fractionation factors from 0 to 300 °C (Table 5).

Table 4
Equilibrium Se isotope fractionation Δ_{A-B} between any two Se species in this paper at 25 °C.

Δ_{A-B}(‰) B A	SeO_2 1.02003	SeO 1.00843	Se_2 1.00562	H_2Se 1.00561	HSe^- 1.00438	$DMSe$ 1.00999	$DMDSe$ 1.00833	$DMSeS$ 1.00872	SeO_4^{2-} 1.03777	SeO_3^{2-} 1.02407	$HSeO_3^-$ 1.02356	$SeMet$ 1.01042	$SeCyst$ 1.01030	$Se(M)^*$ 1.00601	$Se(T)^*$ 1.00595
SeO_2 1.02003	0.0	11.4	14.2	14.2	15.5	9.9	11.5	11.1	−17.2	−3.9	−3.5	9.5	9.6	13.8	13.9
SeO 1.00843		0.0	2.8	2.8	4.0	−1.5	0.1	−0.3	−28.7	−15.4	−14.9	−2.0	−1.9	2.4	2.5
Se_2 1.00562			0.0	0.0	1.2	−4.3	−2.7	−3.0	−31.5	−18.2	−17.7	−4.8	−4.7	−0.4	−0.3
H_2Se 1.00561				0.0	1.2	−4.3	−2.7	−3.1	−31.5	−18.2	−17.7	−4.8	−4.7	−0.4	−0.3
HSe^- 1.00438					0.0	−5.6	−3.9	−4.3	−32.7	−19.4	−18.9	−6.0	−5.9	−1.6	−1.6
$DMSe$ 1.00999						0.0	1.6	1.3	−27.1	−13.8	−13.3	−0.4	−0.3	3.9	4.0
$DMDSe$ 1.00833							0.0	−0.4	−28.8	−15.5	−15.0	−2.1	−2.0	2.3	2.4
$DMSeS$ 1.00872								0.0	−28.4	−15.1	−14.6	−1.5	−1.4	2.7	2.8
SeO_4^{2-} 1.03777									0.0	13.3	13.8	26.7	26.8	31.1	31.3
SeO_3^{2-} 1.02407										0.0	0.5	13.4	13.5	17.8	17.8
$HSeO_3^-$ 1.02356											0.0	12.9	13.0	17.3	17.4
$SeMet$ 1.01042												0.0	0.1	4.4	4.4
$SeCyst$ 1.01030													0.0	4.3	4.3
$Se(M)^*$ 1.00601														0.0	0.0
$Se(T)^*$ 1.00595															0.0

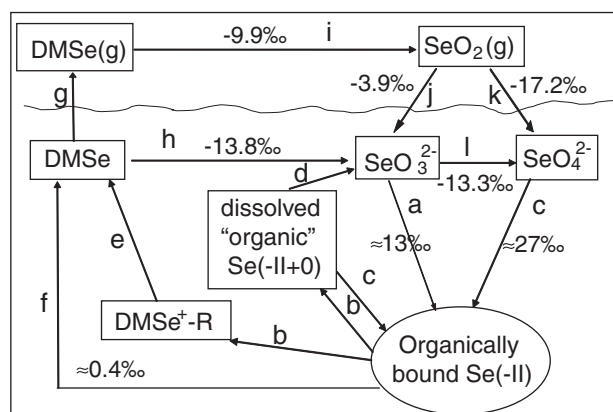*Se(M) denotes monoclinic structure; Se(T) denotes the trigonal one.

Fig. 4. Equilibrium Se isotope fractionation diagram in biogeochemical cycle of selenium based on Fig. 6 in the paper of Cooke and Bruland (1987). (a) reductive assimilation of selenate and selenite into organically bound selenide by organisms; (b) release of organically bound selenide back to solution; (c) assimilation of dissolved organic selenide by organisms; (d) oxidation of dissolved organic selenide to selenite; (e) conversion of dissolved DMSe$^+$-R to dimethyl selenide (DMSe); (f) direct release of DMSe to solution; (g) degassing of DMSe to the atmosphere; (h) oxidation of DMSe to selenite; (i) oxidation of DMSe to SeO$_2$ in atmosphere; (j) conversion of gaseous SeO$_2$ to selenite; (k) conversion of gaseous SeO$_2$ to selenate; and (l) oxidation of selenite to selenate.

4. Discussion

The general trend of enrichment of heavy Se isotopes provided in this study is useful for indicating the change of redox conditions. The Se($-$II) species can preferentially enrich light Se isotopes no matter if it is in organic (e.g. alkylselenides and selenoamino acids) or inorganic forms. If there is a chance that Se(VI) or Se (IV) species can co-exist with Se($-$II) species (e.g. in organic forms), large fractionations can be expected due to the large valence state changes. Se isotopes therefore can be used as tracer of reducing environments because some researchers suggested that the oxidation of Se from low to high valence does not fractionate Se isotopes (Johnson and Bullen, 2004; Johnson et al., 1999, 2000). Some light isotopic compositions of geological samples might reflect the involvements of sulfides or organic matters. It might be used to explain the largest Se isotopic variation found in Yutangba Se deposit, Huber Province, China, the $\delta^{82/76}Se_{NIST}$ values vary from $-12.77‰$ to $4.93‰$ (Wen et al., 2007). The data suggest that reduction reactions might have happened, and light Se isotopes prefer to the organic-rich environments, such as coal and black shales, which can explain the light Se isotopic composition ($-12.77‰$) of carbonaceous shale (Wen et al., 2007).

It is obvious that organisms play an important role in the cycling of Se in the whole ecosystem. Se might be transported and transformed via different chemical and physical pathways. Since biomethylation of Se has been considered as a major pathway in surface waters, the isotope fractionation involving alkylselenides and selenoamino acids will greatly affect Se isotope distributions in ocean surfaces as well as in the atmosphere, eventually the global Se cycling. Without further information about molecular level mechanisms of each pathway, we provide equilibrium Se isotope fractionation factors for each step of biogeochemical cycle of Se in natural waters (Fig. 4). We are not sure if these fractionations are correct because some biochemical processes involving organisms will use "transporters" to exchange elements between bio-materials and the environment. For such situations, the Se fractionation should be re-evaluated by considering the Se bonding forms in those transporters. All in all, our attempting analyses find that the transformation process from inorganic compounds to the organically bound Se seems to lead large rearrangement of Se isotopes (Fig. 4).

5. Conclusions

Equilibrium Se isotope fractionation parameters among some dominant Se species in gaseous, aqueous and condensed phases in nature have been carefully evaluated. Our gaseous Se species data agree with previous results very well. The redox condition is the controlling factor to Se isotope fractionation. Our results suggest a general trend of enrichment of heavy Se isotopes as $SeO_4^{2-} > SeO_3^{2-} > HSeO_3^- > SeO_2 >$ selenoamino acids $>$ alkylselenides $> Se(0)$ or $H_2Se > HSe^-$. The largest fractionation at 25 °C, 33‰, occurs between SeO_4^{2-} and organically bound Se($-$II) if they can coexist. Se($-$II) species will extremely enrich light Se isotopes relative to the high valence states of Se species. Such large isotope fractionations suggest that Se isotopes may be used as an indicator for distinguishing reduction processes, and they might also greatly affect Se isotope distributions in nature. These basic equilibrium Se isotope fractionation factors provided in this study will largely help the field of Se stable isotope geochemistry.

Appendix

In this study, we use a frequency scaling factor (1.05) for the Se isotope fractionation calculation at B3LYP/6-311+G** level. It is because such scaling factor can let the harmonic frequencies match those of much higher levels (i.e. MP2/aug-cc-pVTZ, CCSD/aug-cc-pVTZ and CCSD/aug-cc-pVQZ). Table A1 shows the calculated harmonic frequencies and suggested scaling factors for the B3LYP/6-311+G** level.

Table A1
The calculated harmonic frequencies and suggested scaling factors for B3LYP/6-311+G** level.

	Se$_2$	SeO	H$_2$Se		
B3LYP/6-311+G**	378	891	1071	2379	2396
B3LYP/6-311+G(2df,p)	381	931	1067	2396	2411
(suggested scaling factor)	(1.008)	(1.045)		(1.005)	
CCSD/aug-cc-pVTZ	387	941	1083	2494	2513
(suggested scaling factor)	(1.024)	(1.056)		(1.056)	
CCSD/aug-cc-pVQZ	399	953	1088	2494	2510
(suggested scaling factor)	(1.056)	(1.070)		(1.055)	
MP2/aug-cc-pVTZ	366*	805*	1078	2547	2571
(suggested scaling factor)	(?)	(?)		(1.045)	

Note: There is something obviously wrong for our MP2 calculations of Se$_2$ and SeO. These two data are not used to calibrate the scaling factor of the B3LYP/6-311+G** level.

References

Anbar, A.D., Jarzecki, A.A., Spiro, T.G., 2005. Theoretical investigation of iron isotope fractionation between Fe(H2O)(3+)(6) and Fe(H2O)(2+)(6): implications for iron stable isotope geochemistry. Geochim. Cosmochim. Acta 69, 825–837.
Barone, V., 2004. Vibrational zero-point energies and thermodynamic functions beyond the harmonic approximation. J. Chem. Phys. 120, 3059–3065.
Becke, A.D., 1993. A new mixing of hartreee-fork and local density-functional theories. J. Chem. Phys. 98, 1372–1377.
Bigeleisen, J., Mayer, M.G., 1947. Calculation of equilibrium constants for isotopic exchange reactions. J. Chem. Phys. 15, 261–267.
Burbank, R., 1951. The crystal structure of [alpha]-monoclinic selenium. Acta Crystallogr. 4, 140–148.
Burbank, R., 1952. The crystal structure of [beta]-monoclinic selenium. Acta Crystallogr. 5, 236–246.

Cameron, D.M., Sears, W.C., Nielsen, H.H., 1939. The infra-red absorption by hydrogen selenide, deuterium selenide and deutero-hydrogen selenide. J. Chem. Phys. 7, 994–1002.

Chacko, T., Cole, D.R., Horita, J., 2001. Equilibrium oxygen, hydrogen and carbon isotope fractionation factors applicable to geologic systems. Rev. Mineral. Geochem. 43, 1–81.

Challenger, F., North, H.E., 1934. The production of organ-metalloidal compounds by microorganisms. II. Dimethyl selenide. J. Chem. Soc. 68–71.

Cherin, P., Unger, P., 1967. The crystal structure of trigonal selenium. Inorganic Chemistry 6, 1589–1591.

Cooke, T.D., Bruland, K.W., 1987. Aquatic chemistry of selenium: evidence of biomethylation. Environ. Sci. Technol. 21, 1214–1219.

Cooper, W.C., Bennett, K.G., Croxton, F.C., 1974. The History, Occurrence, and Properties of Selenium. Van Nostrand Reinhold, New Youk.

Criss, R.E., 1999. Principles of Stable Isotope Distribution. Oxford University Press, New York.

Cutter, G.A., 1982. Selenium in reducing waters. Science 217, 829–831.

Dauchy, X., Potin-Gautier, M., Astruc, A., Astruc, M., 1994. Analytical methods for the speciation of selenium compounds: a review. Fresenius J. Anal. Chem. 348, 792–805.

Driesner, T., Seward, T.M., 2000. Experimental and simulation study of salt effects and pressure/density effects on oxygen and hydrogen stable isotope liquid-vapor fractionation for 4–5 molal aqueous NaCl and KCl solutions to 400 degrees C. Geochim. Cosmochim. Acta 64, 1773–1784.

Elrashidi, M.A., Adriano, D.C., Workman, S.M., Lindsay, W.L., 1987. Chemical equilibria of selenium in soils: a theoretical development 1. Soil Sci. 144, 141–152.

Fan, H., Wen, H., Hu, R., Zhang, Y., 2007. Stable isotope of redox-sensitive elements (Se, Cr, Mo). Earth Sci. Front. 14, 264–276.

Fan, T.W.M., Teh, S.J., Hinton, D.E., Higashi, R.M., 2002. Selenium biotransformations into proteinaceous forms by foodweb organisms of selenium-laden drainage waters in California. Aquat. Toxicol. 57, 65–84.

Flury, M., Frankenberger, W.T., Jury, W.A., 1997. Long-term depletion of selenium from Kesterson dewatered sediments. Sci. Total Environ. 198, 259–270.

Frankenberger, W.T., Arshad, M., 2001. Bioremediation of selenium-contaminated sediments and water. Biofactors 14, 241–254.

Frisch, M.J., Trucks, G.W., Schlegel, H.B., Scuseria, G.E., Robb, M.A., Cheeseman, J.R., Montgomery, J.A., Vreven, T., Kudin, K.N., Burant, J.C., Millam, J.M., Iyengar, S.S., Tomasi, J., Barone, V., Mennucci, B., Cossi, M., Scalmani, G., Rega, N., Petersson, G.A., Nakatsuji, H., Hada, M., Ehara, M., Toyota, K., Fukuda, R., Hasegawa, J., Ishida, M., Nakajima, T., Honda, Y., Kitao, O., Nakai, H., Klene, M., Li, X., Knox, J.E., Hratchian, H.P., Cross, J.B., Bakken, V., Adamo, C., Jaramillo, J., Gomperts, R., Stratmann, R.E., Yazyev, O., Austin, A.J., Cammi, R., Pomelli, C., Ochterski, J.W., Ayala, P.Y., Morokuma, K., Voth, G.A., Salvador, P., Dannenberg, J.J., Zakrzewski, V.G., Dapprich, S., Daniels, A.D., Strain, M.C., Farkas, O., Malick, D.K., Rabuck, A.D., Raghavachari, K., Foresman, J.B., Ortiz, J.V., Cui, Q., Baboul, A.G., Clifford, S., Cioslowski, J., Stefanov, B.B., Liu, G., Liashenko, A., Piskorz, P., Komaromi, I., Martin, R.L., Fox, D.J., Keith, T., Al-Laham, M.A., Peng, C.Y., Nanayakkara, A., Challacombe, M., Gill, P.M.W., Johnson, B., Chen, W., Wong, M.W., Gonzalez, C., Pople, J.A., 2003. Gaussian 03 (Revision A.1). Gaussian, Inc, Pittsburgh, PA.

Gibbs, G.V., 1982. Molecules as models for bonding in silicates. Am. Mineralog. 67, 421–450.

Harris, N.J., 1995. A systematic theoretical study of harmonic vibrational frequencies and deuterium isotope fractionation factors for small molecules. J. Phys. Chem. 99, 14689–14699.

Hashimoto, Y., Winchester, J.W., 1967. Selenium in the atmosphere. Environ. Sci. Technol. 1, 338–340.

Hehre, W.J., Radom, L., Schleyer, P.V.R., Pople, J.A., 1986. Ab initio Molecular Orbital Theory. John Wiley and Sons, New York.

Hezberg, G., 1950. Molecular spectra and molecular structure. I. Spectra of diatomic molecules. Van Nostrand Reinhold, New York.

Jarzecki, A.A., Anbar, A.D., Spiro, T.G., 2004. DFT analysis of Fe(H2O)63+ and Fe(H2O)62+ structure and vibrations; implications for isotope fractionation. J. Phys. Chem. A 108, 2726–2732.

Johnson, T.M., 2004. A review of mass-dependent fractionation of selenium isotopes and implications for other heavy stable isotopes. Chem. Geol. 204, 201–214.

Johnson, T.M., Bullen, T.D., 2004. Mass-dependent fractionation of selenium and chromium isotopes in low-temperature environments. Rev. Mineral. Geochem. 55, 289–317.

Johnson, T.M., Bullen, T.D., Zawislanski, P.T., 2000. Selenium stable isotope ratios as indicators of sources and cycling of selenium:results from the northern reach of san francisco bay. Environ. Sci. Technol. 34, 2075–2079.

Johnson, T.M., Herbel, M.J., Bullen, T.D., Zawislanski, P.T., 1999. Selenium isotope ratios as indicators of selenium sources and oxyanion reduction. Geochim. Cosmochim. Acta 63, 2775–2783.

Kajander, E.O., Pajula, R.–L., Harvima, R.J., Eloranta, T.O., 1989. Synthesis and analysis of selenomethionine metabolites. Anal. Biochem. 179, 396–400.

Krouse, H.R., Thode, H.G., 1962. Thermodynamic properties and geochemistry of isotopic compounds of selenium. Can. J. Chem. 40, 367–375.

Lee, C., Yang, W., Parr, R.G., 1988. Development of the Colle–Salvetti correlation-energy formula into a functional of the electron density. Phys. Rev. B 35, 785–789.

Li, X., Zhao, H., Tang, M., Liu, Y., 2009. Theoretical prediction for several important equilibrium Ge isotope fractionation factors and geological implications. Earth Planet. Sci. Lett. 287, 1–11.

Li, X.F., Liu, Y., 2010. First-principles study of Ge isotope fractionation during adsorption onto Fe(III)-oxyhydroxide surfaces. Chem. Geol. 278, 15–22.

Liu, Q., Tossell, J.A., Liu, Y., 2010. On the proper use of the Bigeleisen–Mayer equation and corrections to it in the calculation of isotopic fractionation equilibrium constants. Geochim. Cosmochim. Acta 74, 6965–6983.

Liu, Y., Tossell, J.A., 2005. Ab initio molecular orbital calculations for boron isotope fractionations on boric acids and borates. Geochim. Cosmochim. Acta 69, 3995–4006.

Marsh, R.E., Pauling, L., McCullough, J.D., 1953. The crystal structure of [beta] selenium. Acta Crystallogr. 6, 71–75.

Martin, J.L., Gerlach, M.L., 1969. Separate elution by ion-exchange chromatography of some biologically important selenoamino acids. Anal. Biochem. 29, 257–264.

McConnell, K.P., Wabnitz, C.H., 1957. Studies on the fixation of radioselenium in proteins. J. Biol. Chem. 226, 765–776.

O'Neil, J.R., 1986. Theoretical and experimental aspects of isotopic fractionation. Rev. Mineral. Geochem. 16, 1–40.

Oi, T., 2000. Ab initio molecular orbital calculations of reduced partition function ratios of polyboric acids and polyborate anions. Z. Naturforsch. J. Phys. Sci. 55, 623–628.

Oi, T., Yanase, S., 2001. Calculations of reduced partition function ratios of hydrated monoborate anion by the ab initio molecular orbital theory. J. Nucl. Sci. Technol. 38, 429–432.

Otake, T., Lasaga, A.C., Ohmoto, H., 2008. Ab initio calculations for equilibrium fractionations in multiple sulfur isotope systems. Chem. Geol. 249, 357–376.

Peterson, P.J., Butler, G.W., 1962. The ptake and assimilation of selenite by highter plants. J. Biol. Sci. 15, 126–146.

Redlich, O., 1935. A general relationship between the oscillation frequency of isotropic molecules—(with remarks on the calculation of harmonious force constants). Z. Phys. Chem. Abt. A 28, 371–382.

Richet, P., Bottinga, Y., Javoy, M., 1977. A review of hydrogen, carbon, nitrogen, oxygen, sulphur, and chlorine stable isotope fractionation among gaseous molecules. Annu. Rev. Earth Planet. Sci. 5, 65–110.

Rouxel, O., Ludden, J., Carignan, J., Marin, L., Fouquet, Y., 2002. Natural variations of Se isotopic composition determined by hydride generation multiple collector inductively coupled plasma mass spectrometry. Geochim. Cosmochim. Acta 66, 3191–3199.

Rustad, J.R., Bylaska, E.J., 2007. Ab initio calculation of isotopic fractionation in B(OH)(3)(aq) and BOH4-(aq). J. Am. Chem. Soc. 129, 2222–2223.

Rustad, J.R., Nelmes, S.L., Jackson, V.E., Dixon, D.A., 2008. Quantum-chemical calculations of carbon-isotope fractionation in CO2(g), aqueous carbonate species, and carbonate minerals. J. Phys. Chem. A 112, 542–555.

Rustad, J.R., Zarzycki, P., 2008. Calculation of site-specific carbon-isotope fractionation in pedogenic oxide minerals. Proc. Natl Acad. Sci. USA 105, 10297–10301.

Rustad, J.R., Casey, W.H., Yin, Q.Z., Bylaska, E.J., Felmy, A.R., Bogatko, S.A., Jackson, V.E., Dixon, D.A., 2010. Isotopic fractionation of Mg2+(aq), Ca2+(aq), and Fe2+(aq) with carbonate minerals. Geochim. Cosmochim. Acta 74, 6301–6323.

Schauble, E.A., 2004. Applying stable isotope fractionation theory to new systems. Rev. Mineral. Geochem. 55, 65–111.

Schauble, E.A., 2007. Role of nuclear volume in driving equilibrium stable isotope fractionation of mercury, thallium, and other very heavy elements. Geochim. Cosmochim. Acta 71, 2170–2189.

Schauble, E.A., Ghosh, P., Eiler, J.M., 2006. Preferential formation of C-13–O-18 bonds in carbonate minerals, estimated using first-principles lattice dynamics. Geochim. Cosmochim. Acta 70, 2510–2529.

Schauble, E.A., Rossman, G.R., Taylor, H.P., 2003. Theoretical estimates of equilibrium chlorine-isotope fractionations. Geochim. Cosmochim. Acta 67, 3267–3281.

Seo, J.H., Lee, S.K., Lee, I., 2007. Quantum chemical calculations of equilibrium copper(I) isotope fractionations in ore-forming fluids. Chem. Geol. 243, 225–237.

Sun, M.S., Weege, R.J., 1959. Native selenium from Grants, New-Mexico. Am. Mineralog. 44, 1309–1311.

Suzuki, K.T., Doi, C., Suzuki, N., 2008. Simultaneous tracing of multiple precursors each labeled with a different homo-elemental isotope by speciation analysis: distribution and metabolism of four parenteral selenium sources. Pure Appl. Chem. 80, 2699–2713.

Thompson, M.E., Roach, C., Braddock, W., 1956. New occurrences of native selenium. Am. Mineralog. 41, 156–157.

Urey, H.C., 1947. Thermodynamic properties of isotopic substance. J. Chem. Soc. 562–581.

Wen, H., Carignan, J., 2007. Reviews on atmospheric selenium: emissions, speciation and fate. Atmos. Environ. 41, 7151–7165.

Wen, H., Carignan, J., Hu, R., Fan, H., Chang, B., Yang, G., 2007. Large selenium isotopic variations and its implication in the Yutangba Se deposit, Hubei Province, China. Chin. Sci. Bull. 52, 2443–2447.

Zeebe, R.E., 2005. Stable boron isotope fractionation between dissolved B(OH)(3) and B(OH)(4)(−). Geochim. Cosmochim. Acta 69, 2753–2766.

Zeebe, R.E., 2010. A new value for the stable oxygen isotope fractionation between dissolved sulfate ion and water. Geochim. Cosmochim. Acta 74, 818–828.

Zhu, J.M., Liang, X.B., Zheng, B.S., Li, S.H., 2002. Occurrence of native selenium in Yutangba of China. Geochim. Cosmochim. Acta 66, A880-A880.

Zhu, J.M., Zheng, G.D., Johnson, T.M., Li, S.H., 2005. Distribution of native selenium in Yutangba of China and its environmental implications. Geochim. Cosmochim. Acta 69, A193-A193.

Zhu, J.M., Zuo, W., Liang, X.B., Li, S.H., Zheng, B.S., 2004. Occurrence of native selenium in Yutangba and its environmental implications. Appl. Geochem. 19, 461–467.